Lattice-Geometry Effects in Garnet Solid Electrolytes from Lattice-Gas Monte Carlo Simulations

Benjamin J. Morgan[1]

[1] *Department of Chemistry, University of Bath, Claverton Down, Bath, BA2 7AY*

(Dated: June 12, 2017)

In many solid electrolytes, ion transport can be approximated as a sequence of hops between distinct lattice sites. Assuming these hops are uncorrelated allows quantitative relationships to be derived between microscopic hopping rates and macroscopic transport coefficients; tracer diffusion coefficients and ionic conductivities. In real materials, the assumption of uncorrelated hops is exact only in the dilute limit, where interactions between mobile ions can be neglected. At non-dilute concentrations these interactions can be significant, and ion hops become correlated. This causes the relationships between hopping frequency, diffusion coefficent, and ionic conductivity to deviate from the random walk expressions, with this effect quantified by single-particle and collective correlation factors, f and f_I. These parameters differ between materials, and depend on the concentration of mobile particles, the nature of the interactions, and the host lattice geometry. Here we study these correlation effects for the garnet lattice using lattice-gas Monte Carlo simulations. This lattice describes diffusion pathways in lithium-garnets—a family of promising solid lithium-ion electrolytes—and has an unusual geometry containing both 4-coordinate and 2-coordinate sites. We find that for non-interacting particles (volume exclusion only) single-particle correlation effects are more significant than for any other 3D solid electrolyte lattice. This is attributed to the presence of 2-coordinate lattice sites, which gives correlation effects intermediate between typical 3D and 1D lattices. Including nearest-neighbour repulsion and on-site energy differences gives more complex single-particle correlation behaviour and introduces collective correlation effects. In particular, we find strong correlation effects at $x(\mathrm{Li}) = 3$ (site energies) and $x(\mathrm{Li}) = 6$ (nearest-neighbour repulsion). Both effects correspond to ordering of the mobile particles over the lattice. Finally we consider the question of how mobile ion stoichiometry can be tuned to maximise the ionic conductivity. We find the optimal stoichiometry is highly sensitive to the choice of interaction parameters.

I. INTRODUCTION

The ability of solid electrolytes to conduct electric charge by transporting ions is central to their use in devices such as fuel cells and solid-state lithium-ion batteries.[1–4] In both cases, solid electrolytes with high ionic conductivities are desirable. In fuel cells high conductivities allow lower operating temperatures, reducing running costs and increasing operating lifetimes. In solid-state batteries high conductivities allow faster charging rates and higher power output. Ionic conductivities depend on a number of factors, including the crystal structure, the chemical composition, and the concentration of mobile ions.[5] Developing a quantitative understanding of these factors is key to developing high ionic conductivity solid electrolytes for use in high performance electrochemical devices.

Solid electrolytes can be considered to comprise two distinct sets of ions: "fixed" ions that vibrate about their crystallographic sites, and "mobile" ions that diffuse through the system and contribute to ionic conductivity. The fixed ion positions define a network of diffusion pathways through which the mobile ions can move. Families of solid electrolytes with common crystal structures therefore have topologically equivalent diffusion networks, while electrolytes with different crystal structures will have topologically distinct diffusion paths. While much research into solid electrolytes focusses on understanding differences in ionic conductivities within specific structural families, a complementary question considers how differences in crystal structure, and hence diffusion network topology, affect ionic transport.

Crystal structure can be considered a microscopic characteristic, dictating the positions of individual atoms. Ionic transport at scales relevant to device performance, however, is described by macroscopic transport coefficients: diffusion coefficients and ionic conductivities. These describe long-time behaviours, and represent ensemble averages over all microscopic diffusion processes. A meaningful understanding of differences in ionic conductivity between solid electrolytes therefore depends on the quantitative relationships between microscropic diffusion and macroscopic ion transport.

In many solid electrolytes, the microscopic transport of ions can be approximated as a sequence of discrete "hops" between distinct lattice sites.[6] If these hops are *independent*, every ion follows a random walk. The tracer diffusion coefficient, D^*, and ionic conductivity, σ, can then be expressed in terms of the average hop-rate per atom, $\widetilde{\nu}$,[7] via[8,9]

$$D^* = \frac{1}{6} a^2 \widetilde{\nu}; \tag{1}$$

$$\sigma = \frac{Cq^2}{kT} \frac{1}{6} a^2 \widetilde{\nu}; \tag{2}$$

where a is the characteristic hop distance, C is the mobile ion concentration, and q is the charge of the mobile ions.

Equations 1 and 2 can be combined to give the "Nernst-Einstein relation", which connects D^* and σ:

$$\frac{\sigma}{D^*} = \frac{Cq^2}{kT}. \tag{3}$$

These three equations describe quantitative relationships between the hop-rate, $\widetilde{\nu}$, tracer diffusion coefficient, D^*, and ionic conductivity, σ. Their derivation, however, depends on the assumption that all hops are independent, which holds only in the limit of very low carrier concentrations, or for fully non-interacting mobile ions.[10]

Practical solid electrolytes typically have high carrier concentrations, and interparticle interactions can be significant. In these cases, individual hop probabilities depend on the specific arrangement of nearby ions, and hops are no longer statistically independent. Instead, ion trajectories are *correlated*, and deviate from the random walk behaviour of non-interacting systems.[8,11–13] Correlations between hops made by individual ions modify the relationship between average hop rate, $\widetilde{\nu}$, and tracer diffusion coefficient, D^*, which becomes

$$D^* = \frac{1}{6}a^2\widetilde{\nu}f, \tag{4}$$

where f is a single-particle correlation factor that accounts for the deviations from random walk behaviour. Correlations between hops made by *different* ions modify the relationship between $\widetilde{\nu}$ and σ, which becomes

$$\sigma = \frac{Cq^2}{kT}\frac{1}{6}a^2\widetilde{\nu}f_{\mathrm{I}}, \tag{5}$$

where f_{I} is a collective or "physical" correlation factor.[10,14,15] The relationship between σ and D^* now differs from Nernst-Einstein behaviour (Eqn. 3) by the ratio of these correlation factors:

$$\frac{\sigma}{D^*} = \frac{Cq^2}{kT}\frac{f_{\mathrm{I}}}{f}. \tag{6}$$

The inverse ratio $\frac{f}{f_{\mathrm{I}}}$ is commonly denoted as the Haven ratio, H_{R}[10,16].

Quantitative relationships between microscopic hopping rates and macroscopic transport coefficients can, in principle, be obtained by combining experimental data for $\widetilde{\nu}$, D^*, and σ. Ion hopping rates may be measured from NMR or muon spin-relaxation experiments,[17–22] diffusion coefficients obtained from tracer diffusion experiments,[23] and ionic conductivities derived via impedence spectroscopy.[24,25] Computational methods provide an increasingly used alternative to direct experimental studies. First principles calculations of barrier heights and vibrational partition functions along diffusion pathways give hopping rates.[26,27] Molecular dynamics simulations can be used to directly calculate tracer diffusion coefficients and ionic conductivities.[28] Often, however, it is convenient, or necessary, to use one member of $\{\widetilde{\nu}, D^*, \sigma\}$ to calculate the others. All three parameters might not be known under equivalent experimental conditions, or one wishes to compare results from complementary approaches. Because the quantitative relationships between $\{\widetilde{\nu}, D^*, \sigma\}$ depend on f and f_{I} (and their ratio H_{R}), it is important to know these correlation factors for the materials under consideration.

For many simple crystal lattices the correlation parameters $\{f, f_{\mathrm{I}}, H_{\mathrm{R}}\}$ have been calculated.[10,29] For more complex crystal structures, however, these parameters are unknown. It is therefore common for studies to use the simplified Eqns. 1, 2, 3 to convert between $\{\widetilde{\nu}, D^*, \sigma\}$. This is equivalent to assuming non-interacting behaviour, where $f = 1, f_{\mathrm{I}} = 1, H_{\mathrm{R}} = 1$. For materials where correlations are significant, this can introduce quantitative errors.

In this study, we focus on quantifying these relationships for garnet-structured solid electrolytes. The "lithium-garnets" are a family of solid lithium-ion electrolytes $\mathrm{Li_xM_3M'_2O_{12}}$,[30,31] that have attracted significant attention as candidates for all–solid-state lithium-ion batteries.[1,32] The garnet crystal structure has an unusual three-dimensional network of lithium diffusion pathways, consisting of interlocking rings.[33] Each ring comprises 12 alternating tetrahedral and octahedral sites, with the tetrahedral sites acting as nodal points connecting adjacent rings (Fig. 1). Aliovalent substitution of the M and M' cations allows the lithium stoichiometry to be tuned across a broad range. A lithium stoichiometry of $x_{\mathrm{Li}} = 9$ corresponds to a fully occupied lithium-site lattice, and research has focussed on "lithium stuffed" garnets, typically with $x_{\mathrm{Li}} = 5 \rightarrow 7$. Ionic conductivities vary enormously as a function of x_{Li}, with σ increasing by $\sim 10^9$ between $\mathrm{Li_3Ln_3Te_2O_{12}}$ and $\mathrm{Li_{6.55}La_3Zr_2O_{12}}$,[1,31] and it remains an open question precisely how the lithium diffusion coefficient and ionic conductivity vary with lithium stoichiometry. It is also not know to what extent the unusual diffusion pathway topology affects ionic transport. Resolving these questions is critical for the optimisation of ionic conductivity for this family of materials.

Theoretical considerations and published data indicate that lithium distribution and transport in lithium garnets exhibit significant correlation effects. The relationship between lithium stoichiometry and lithium transport coefficients is therefore expected to be non-ideal. Low coordination numbers for the lithium lattice-sites: 4 for tetrahedra and 2 for octahedra; suggest significant site-blocking effects.[33] Short distances of ~ 2.4 Å between lithium sites suggest strong Li–Li Coulomb repulsion, becoming increasingly significant at high Li content.[34–37] The presence of two non-equivalent sets of lattice sites is a further factor: if ideally distributed, lithium ions would occupy the octahedral and tetrahedral lattice sites in a 2:1 ratio at all Li concentrations. Neutron data however show that at low lithium content ($x_{\mathrm{Li}} = 3$) only tetrahedral sites are occupied,[38] while at higher lithium content ($x_{\mathrm{Li}} = 5 \rightarrow 7$) octahedral sites become preferentially occupied.[31,36] Experimental conduc-

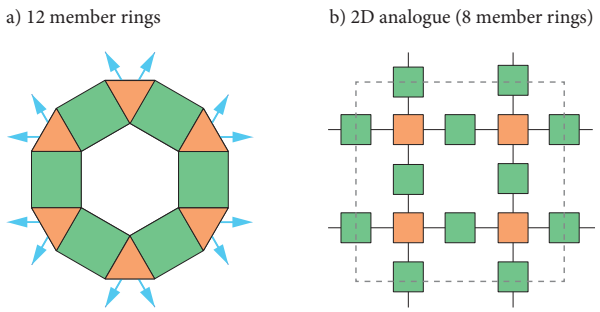

FIG. 1. Schematic of the ring structures that constitute the garnet lithium-diffusion network. a) Each ring consists of 12 alternating tetrahedra (orange) and octahedra (blue). Arrows show connections to neighbouring rings.[33] b) A 2D analogue of interconnected 8-membered rings of alternating "tetrahedra" and "octahedra".

tivities have also been found to show non-linear dependence on x_{Li},[39] and to deviate strongly from ideal values predicted (via Eqn. 2) from muon-spin–spectroscopy hopping rates.[21] Further evidence for correlated transport in lithium garnets has been provided by computational studies. Molecular dynamics simulations have been used to identify a variety of correlated diffusion processes,[40–43] while calculated diffusion coefficients and ionic conductivities show non–Nernst-Einstein behaviour ($H_{\mathrm{R}} < 1$).[44,45] The quantitative effects of correlation in lithium garnets, however, are not known, and conversions between hop rates, diffusion coefficients, and ionic conductivities are often approximated by assuming uncorrelated motion.[21,22,24,40,46–54]

To quantitatively describe the relationship between lithium stoichiometry and ionic conductivity in lithium-ion garnets, it is essential to consider non-ideal distributions and transport of the lithium ions. Here we present a computational analysis of these issues, using lattice-gas kinetic Monte Carlo simulations of diffusion on a garnet lattice, for a range of model Hamiltonians. We calculate f and f_{I} as functions of carrier concentration (Li stoichiometry), first for a non-interacting volume-exclusion model,[55] and then for models that include on-site single-particle energies and/or nearest-neighbour repulsion interactions. In addition to self- and collective-correlation factors, we present site occupation populations, diffusion coefficients, and effective ionic conductivities for this range of simulation models, allowing us to discuss how different interactions contribute to non-ideal behaviour, and modify the relationships between particle hopping rate, diffusion coefficient, and ionic conductivity.

We find that for non-interacting particles (volume exclusion only) single-particle correlation effects are more significant than for any other 3D solid electrolyte lattice. This is attributed to the presence of 2-coordinate lattice sites, which gives correlation effects intermediate between typical 3D and 1D lattices. Including nearest-neighbour repulsion and on-site energy differences gives more complex single-particle correlation behaviour and introduces collective correlation effects. In particular, we find strong correlation effects at $x(\mathrm{Li}) = 3$ (site energies) and $x(\mathrm{Li}) = 6$ (nearest-neighbour repulsion). Both effects correspond to ordering of the mobile particles over the lattice. Finally we consider the question of how mobile ion stoichiometry can be tuned to maximise the ionic conductivity. We find the optimal stoichiometry is highly sensitive to the choice of interaction parameters.

II. METHODS

Lattice-gas Monte Carlo simulations describe the diffusion of a set of mobile ions populating some host lattice, expressed as a graph of interconnected sites. Every lattice site is either occupied or vacant, and during a simulation the mobile ions undergo a sequence of hops from site to site. These hops are randomly selected, with relative probabilities that satisfy the principle of detailed balance and represent the underlying model Hamiltonian. The simplest model considered here is a "non-interacting" volume-exclusion–only model.[56] Double occupancy of sites is forbidden, and allowed hops are all equally likely. Non-interacting models allow the pure geometric effect of the lattice to be evaluated, but neglect other interactions that may be significant in corresponding experimental systems. For the garnet lattice, here we also consider the effect of nearest-neighbour interactions between mobile ions, described by a nearest-neighbour repulsion energy, E_{nn}, and interactions between single ions and the lattice, described by on-site energies for tetrahedral versus octahedral sites, E_{T}, E_{O}. The energy of any configuration of occupied sites, j is given by

$$E = \sum_j n_j^{\mathrm{nn}} E_{\mathrm{nn}} + E_{\mathrm{site}}^j, \tag{7}$$

where n_j^{nn} is the number of occupied nearest neighbour sites for (occupied) site j. For interacting systems, the relative probability of hop i depends on the change in total energy ΔE_i for the system if this hop was selected:

$$P_i \propto \begin{cases} \exp\left(\frac{\Delta E_i}{kT}\right), & \text{if } \Delta E_i > 0 \\ 1, & \text{otherwise.} \end{cases} \tag{8}$$

For our interacting systems, the change in energy for each candidate hop can depend on the change in number of nearest-neighbour interactions and the change in on-site energy for moving from a tetrahedral to octahedral site (or vice versa):

$$\Delta E_i = \Delta n_{\mathrm{nn}} E_{\mathrm{nn}} + \Delta E_{\mathrm{site}}. \tag{9}$$

At each simulation step, one hop is randomly selected according to the set of relative probabilities. The corresponding ion is moved, and a new set of relative hop probabilities is generated for the subsequent step.

In the limit of a large number of hops, the tracer- and collective-correlation factors can be evaluated as

$$f = \frac{\sum_i \langle R^2 \rangle}{Na^2}, \tag{10}$$

where $\langle R^2 \rangle$ is the mean-squared displacement of the mobile ions, and N is the total number of hops during the simulation, and

$$f_\mathrm{I} = \frac{|\sum_i R_i|^2}{Na^2}, \tag{11}$$

where $\sum_i R_i$ is the *net* displacement of all mobile particles. In both cases the denominators correspond to the limiting behaviour for uncorrelated diffusion.

To allow time-dependent properties to be evaluated, we perform our lattice-gas Monte Carlo simulations within a rejection-free kinetic Monte Carlo scheme[57]. For each simulation step, k, the set of hop probabilities, $\{P_{i,k}\}$, are converted to rates, $\{\Gamma_{i,k}\}$ by scaling by a common prefactor of $10^{13}\,\mathrm{s}^{-1}$. After selecting a hop, the simulation time is updated by $\Delta t = Q_k^{-1} \ln(1/u)$, where Q_k is the "total rate"; $Q_k = \sum_i \Gamma_{i,k}$, and u is a uniform random number $u \in (0, 1]$. This approach provides time-averaged site occupations, and directly calculated diffusion coefficients and ionic conductivities.

Our lattice-gas kinetic Monte Carlo simulations were performed using the `lattice_mc` code.[58] Simulations were performed for an ideal cubic $2 \times 2 \times 2$ garnet lattice, with 384 octahedral sites and 192 tetrahedral sites. The lattice site coordinates were generated from the cubic high-temperature $Li_7La_3Zr_2O_{12}$ (LLZO) structure (ICSD #422259),[33] with the centres of octahedra and tetrahedra defined by the oxygen sub-lattice used to define the corresponding site coordinates. In cubic LLZO, each lithium-octahedron contains a "split" pair of distorted 96*h* sites, separated by 0.81 Å. The construction used here considers each octahedron as a single ideal 48*g* site. The network of diffusion pathways includes connections between nearest-neighbour sites only, i.e. all connections are between neighbouring tetrahedral–octahedral pairs. [CALCULATED DIFFUSION COEFFICIENTS ARE PRESENTLY IN $\mathrm{bohr}^2\,\mathrm{s}^{-1}$.] For each simulation, n_Li mobile ions are randomly distributed across the lattice sites. 1,000 equilibration steps are performed before 10,000 production steps.

For each set of model parameters, $\{E_\mathrm{nn}, \Delta E_\mathrm{site}\}$, simulations were performed across the full range of possible lithium stoichiometry ($x_\mathrm{Li} = 9$ corresponds to $n_\mathrm{Li} = 576$). For each system, data were collected as an average over 5,000 trajectories.

III. RESULTS

A. Non-Interacting Particles and Geometric Effects

We first examine the pure geometric effect of the garnet lattice by modelling non-interacting systems, for which deviations from random walk behaviour emerge purely from volume exclusion effects. Fig. 2 shows the calculated self- and collective-correlation factors, f and f_I, average tetrahedral and octahedral site occupations, n_tet and n_oct, tracer and "jump" diffusion coefficients, D^* and D_J, and effective (reduced) ionic conductivity, σ', for the volume-exclusion–only simulations, as a function of x_Li.

In the single particle limit, $x_\mathrm{Li} \to 0$, there are no blocking effects, and particles follow a random walk. With increasing concentration of mobile ions, however, single particle diffusion increasingly deviates from random walk behaviour. The tracer correlation factor, f, decreases from $f = 1$ in the single particle limit $x_\mathrm{Li} \to 0$ to $f = 0.25$ in the single vacancy limit $x_\mathrm{Li} \to 9$, with approximately linear dependence on x_Li[59].

The magnitude of the tracer correlation effect for different lattice geometries can characterised by considering f in the limit of a single vacancy, f_v. For the garnet lattice this is the limit $x_\mathrm{Li} \to 9$. Table I presents f_v values previously calculated for common 3D lattices,[60] and for a 1D chain,[14] alongside our value for the garnet lattice. For the garnet lattice, $f_v = 0.25$. This is smaller than for all of the other 3D lattices, by at least a factor of 2, corresponding to unusually strong correlation effects. This result can be understood as a consequence of the particular garnet lattice geometry. For a general set of 3D lattices, as the number of nearest neighbours of each lattice site, z, decreases, f_v also decreases, and correlation effects become more significant. The garnet lattice has both 4-coordinate (tetrahedral) and 2-coordinate (octahedral) sites, and long ranged diffusion follows an alternating T→O→T→O pattern. The calculated value of $f_v = 0.25$ is halfway between the values for the 4-coordinate diamond lattice ($f_v = 0.5$) and for a 1-D chain, where every site is 2-coordinate ($f_v = 0$). This suggests that the extreme low value of f_v for the garnet lattice is a consequence of the low coordination of the lattice sites, in particular the local 1D coordination at the octahedral sites, which act as bottlenecks for long-ranged diffusion.

Lattice	z	f_v
Face centered cubic[60]	12	0.78146
Body centred cubic[60]	8	0.72722
Simple cubic[60]	6	0.65311
Diamond[60]	4	0.5
Garnet [This work]	4+2	0.25
1D chain[14]	2	0.0

TABLE I. Vacancy correlation factors for some common crystal lattices. z is the number of nearest neighbours for each site in the lattice.

For any non-interacting system, the hops made by different particles are unocorrelated, and $f_I = 1$ for all x_Li, making $H_\mathrm{R} = f$. There are also no correlations between site occupations, and the mobile particles are randomly distributed over the available octahedral and tetrahedral

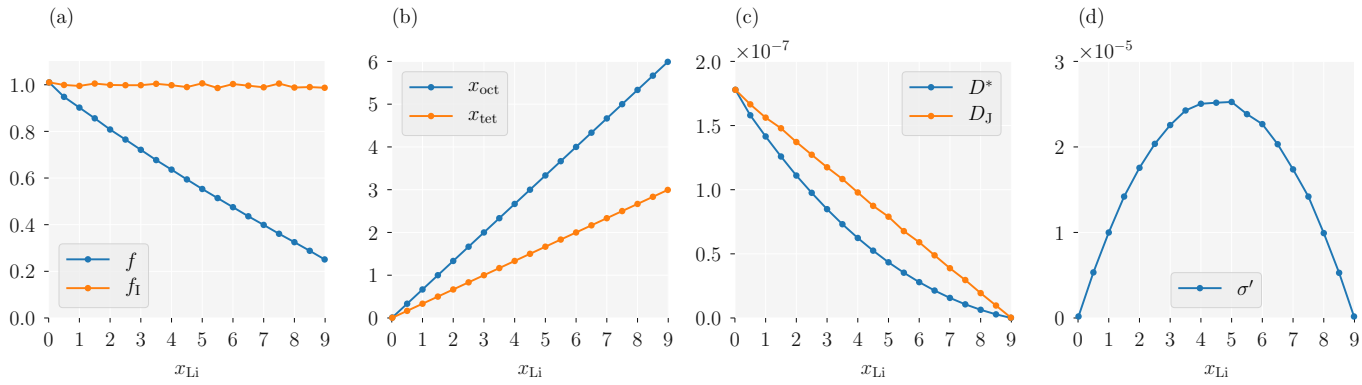

FIG. 2. Non-interacting particles on a garnet lattice: (a) The single-particle correlation factor, f, and collective correlation factor, f_I; (b) Average octahedral and tetrahedral site occupations per forumla unit, x_{oct} and x_{tet} c) Tracer diffusion coefficient, D^*, and "jump" diffusion coefficient D_J. d) Effective ionic conductivity, σ'.

sites, with a 2:1 population ratio that reflects the underlying lattice geometry.

We also consider three measures of ionic transport in this system.[61] Fig. 2(c) shows the tracer diffusion coefficient, D^* (Eqn. 4) and the "jump diffusion coefficient", D_J[5], calculated as

$$D_J = \frac{|\sum_i R_i|^2}{6Nt}. \tag{12}$$

At a fixed temperature D_J is proportional to the mobility, and measures the ease with which the mobile particles undergo collective migration. Both D^* and D_J decrease monotonically from $x_{Li} = 0$ to $x_{Li} = 9$ ($x = 0 \rightarrow 1$), as the number of vacancies available for mobile particles to hop to decreases. For the non-interacting system there are no correlations between hops made by different particles, and the jump diffusion coefficient is proportional to $(1 - x)$.[5,56] [THIS IS NOW x WITH A MAXMIMUM OF 1, I.E. CONCENTRATION]. The tracer diffusion coefficient, however, shows the effect of correlations between hops made by individual particles, and varies according to $D^* \propto (1 - x)f$. The ionic conductivity of a system depends on both the charge-carrier concentration, and the ionic mobility (which is proportional to D_J). To examine the relationship between carrier concentration and *relative* ionic conductivities, we also con consider a "reduced" conductivity, σ',[62] given by

$$\sigma' = xD_J. \tag{13}$$

For any non-interacting system, $\sigma' \propto x\,(1 - x)$, with a maximum at $x = 0.5$ (Fig. 2(d)).

B. Interacting Particles

The conceptual simplicity of the non-interacting system makes it a convenient starting point for understanding the factors affecting ionic transport in different lattices. In real Li-garnet materials, however, interactions between lithium ions, or between lithium ions and the host lattice, can be significant. Lithium ions carry positive charge, and can be expected to experience mutual Coulomb repulsion, and the different oxygen-coordination environments of octahedral and tetrahedral sites can be expected to produce a preference for occupation by lithium at one site versus the other. Within the lattice-gas Monte Carlo scheme, we consider these two factors by introducing, first, nearest-neighbour repulsion, and second, an octahedral versus tetrahedral site preference.

[MOVE THIS COMMENT TO THE INTRODUCTION OR/AND THE DISCUSSION?: SIMULATIONS OF OTHER LATTICE GEOMETRIES WHERE NEAREST-NEIGHBOUR REPULSION HAS BEEN MODELLED PREDICT PARTICLE ORDERING AT SPECIFIC LATTICE OCCUPATION FRACTIONS (DEPENDENT ON THE LATTICE GEOMETRY UNDER CONSIDERATION) AND IS ASSOCIATED WITH STRONG SELF- AND COLLECTIVE-CORRELATION EFFECTS.]

1. *Nearest-Neighbour repulsion*

To examine the effect of Li–Li repulsion, we consider a simplified model with only nearest-neighbour repulsion. The energy of Li at each specific site now depends on the number of occupied neighbouring sites and individual hop probabilities now depend on whether they increase or decrease the total number of nearest-neighbour pairs. Fig. => plot of f, f_I, H_R, n_{tet}, n_{oct}, σ'. presents results of LGMC simulations performed for $E_{nn} = 0.0$–$3.0\,kT$.

Repulsive nearest-neighbour interactions disfavour simultaneous occupation of adjacent sites, and promote ordering of particles across alternating occupied–vacant–occupied–vacant sites. This ordering causes the single-particle correlation behaviour to deviate from that of the non-interacting system, and introduces collective correlations between the mobile ions. In a lattice with only one crystallographic site complete ordering would occur at half–site-occupancy, corresponding to $x_{Li} = 4.5$ for

the garnet lattice. The behaviour of f and f_I with increasing E_nn approximately follow this prediction. Both correlation factors have their non-interacting values in the empty and fully-occupied lattice limits $x \to 0, x \to 1$ and decrease at intermediate stoichiometries. Both correlation factors also show a strong decrease at $x_\mathrm{Li} = 6$, and this is a consequence of the existence of two non-equivalent sites in the garnet lattice.

The garnet lattice consists of octahedral and tetrahedral sites in a 2:1 ratio, with corresponding site occupations for the non-interacting system (Fig. 2(b)). With non-zero nearest-neighbour repulsion, this preference for octahedral sites is reinforced by the preference for alternating occupied–unoccupied sites. Given that octhedral site occupation is entropically favoured, any non-dilute population of particles can minimise its energy by occupying *only* octahedral sites. This effect is strongest at two-thirds site occupation ($x_\mathrm{Li} = 6$) where the octahedral sites are fully occupied and the tetrahedral sites are fully vacant. In this fully ordered system, correlation effects are maximised: any O→T hop by a single particle is likely to be quickly reversed, and diffusion is possible only for highly correlated collective movement by groups of particles[43]. This effect is visible in the effective conductivity, σ', which drops sharply at $x_\mathrm{Li} = 6$.

[Kozinsky *et al.* have also proposed a fully ordered phase at $x_\mathrm{Li} = 6$, from first-principles calculations and group theory analysis, that differs from the pure octahedral occupation described here[63]. The fully-ordered configuration observed here at $x_\mathrm{Li} = 6$ is different from that proposed by Kozinsky *et al.*[63] . That work predicted mixed occupation of octahedral and tetrahedral sites. In that case connected to symmetry breaking / in this case the cubic lattice symmetry is maintained]

2. *Site asymmetry*

The non-interacting model, discussed above, assumes that mobile Li ions show an equal preference for octahedral and tetrahedral sites: the site "type" is only relevant in that it defines the connectivity of each site within the lattice graph. This symmetry in on-site energies means the populations of occupied octahedral and tetrahedral sites simply follow a 2:1 ratio. In experimental Li-garnet samples with $x(Li) = 3$, e.g. $Li_3Y_3Te_2O_{12}$, the lithium ions exclusively occupy the tetrahedral sites[38]. This suggests that in the absence of other interactions, there is an energetic penalty for occupying octahedral rather than tetrahedral sites. We denote this energy cost $\Delta E_\mathrm{site} = E_\mathrm{oct} - E_\mathrm{tet}$. In the following the describe LGMC simulations for otherwise non-interacting particles, with $\Delta E_\mathrm{site} = 0$—$5kT$.

With increasing ΔE_site, tetrahedral sites are preferentially occupied with respect to octahedral sites: at higher values of ΔE_site all lithium ions preferentially occupy tetrahedral sites, with octahedral sites only occupied for $x_\mathrm{Li} > 3$ when the tetrahedral sites are fully occupied. In the limit of $\Delta E_\mathrm{site} \to \infty$ (equivalent to $T \to 0$) x_Li corresponds to an ordered arrangement with all the tetrahedral sites occupied and all the octahedral sites vacant. The preferential tetrahedral occupation and associated ordering correlates with an increased single particle correlation (decreased f) and introduces collective correlation across the full Li stoichiometry range, with the largest effect (smallest $f_m I$) at $x_\mathrm{Li} = 3$. The result that the Li preferentially order for specific numbers of occupied sites, and that this is assocated with strong single-particle and collective correlation effects is consistent with equivalent results obtained for other lattices for which the effect of alternating site energies have been modelled => e.g. refs and examples? 2D hexagonal lattice The Haven ratio, H_R, is slightly decreased relative to the non-interacting case for $x_\mathrm{Li} < 3$, and approximately follows the non-interacting behaviour for $x_\mathrm{Li} > 3$.

3. *Combined site inequality and nearest-neighbour repulsion*

In real Li-garnet materials, both site inequality and Li–Li repulsion can be expected to play a role. We have also performed simulations with both parameters. The low computational cost of LGMC simulations allows the $\{x_\mathrm{Li}, \Delta E_\mathrm{site}, E_\mathrm{nn}\}$ parameter space to be mapped. The simulation data from these calculations are included in the SI / Appendix, and are available as a data set. => include example of both parameters varying, e.g. $\Delta E_\mathrm{site} = 3.0\,\mathrm{eV}$, $E_\mathrm{nn} = 3.0\,\mathrm{eV}$. Introduces "correlation" features at $x = 3, 6$.

Much research in Li-garnets concerns optimising the composition so that the ionic conductivity is maxmimised. Part of this is identifying the Li concentration that maximises the ionic conductivity of this family of materials. => who has proposed arguments for improving ionic conductivity by tuning x_Li?

$$\sigma_\mathrm{dc} \propto c\,(1-c)\,f_\mathrm{I} \tag{14}$$

[is this discussed by anyone? cf. Kutner[56] Behaviour in non-interacting case is described by Kutner. Interactions (between particles or with the lattice) introduce an additional scaling f_I which describes the efficiency with which diffusive jumps contribute to collective transport.] σ_dc is proportional to three terms: the => rewrite this in notation consistent with what appeared earlier The $c(1-c)$ factor gives a parabolic dependence with a maximum ionic conductivity as $x = \frac{9}{2}$, as seen (above?) for the non-interacting / equivalent sites system. By "switching on" additional physics: on-site energies and interactions between mobile ions, $f_\mathrm{I} \neq 1$, with f_I a function of the interaction strengths, the lattice topology, and the carrier concentration. The optimal x_Li for a given material therefore depends on the behaviour of $f_\mathrm{I}(x_\mathrm{Li})$.

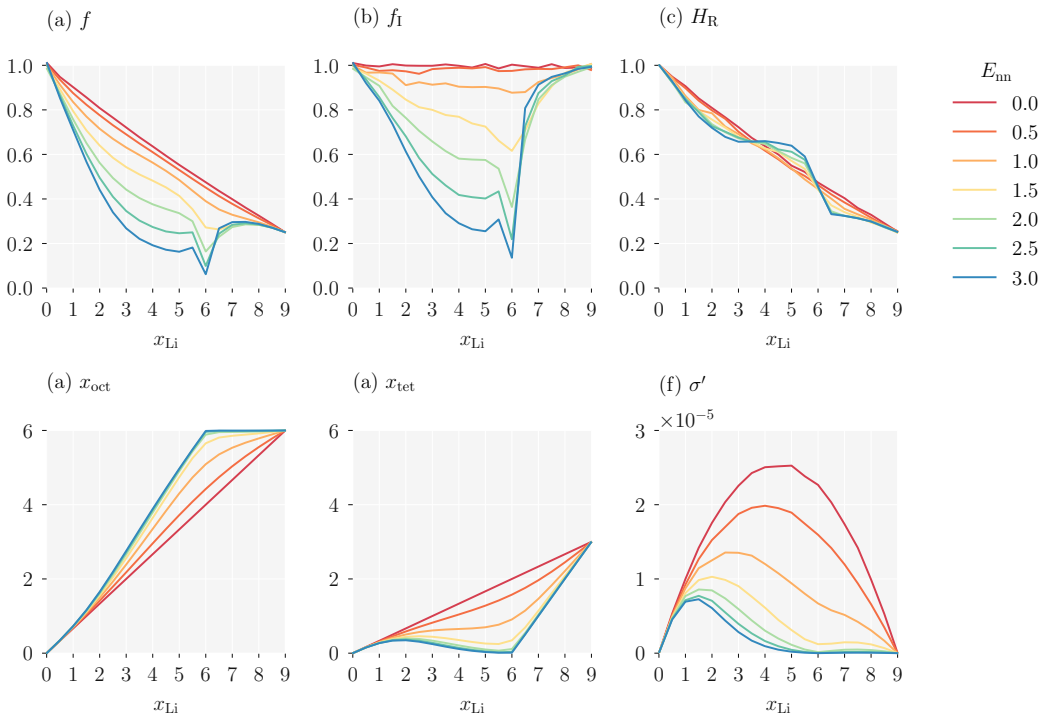

FIG. 3. The effect of nearest-neighbour repulsion between mobile particles on a garnet lattice: (a) single-particle correlation factor, f; (b) collective correlation factor, f_{I}; (c) Haven ratio, H_{R}; (d) average octahedra occupation, x_{oct}; (e) average tetrahedra occupation, x_{tet}; (f) effective ionic conductivity, σ'. E_{nn} is in multiples of kT.

The low computational cost of the LGMC simulations have allowed us to calculate an effective ionic conductivity σ' as a function of $\{x_{\mathrm{Li}}, \Delta E_{\mathrm{site}}, E_{\mathrm{nn}}\}$. Considering this data set, we can pose the following question: what is the value of x_{Li} that maximises the (effective) ionic conductivity, at each combination of $\Delta E_{\mathrm{site}}, E_{\mathrm{nn}}$

At any combination of $\Delta E_{\mathrm{site}}, E_{\mathrm{nn}}$ we can identify the x_{Li} that gives the maximum ionic conductivity, and then map how $\arg\max \sigma'(x_{\mathrm{Li}})$ depends on the scale of interactions. This defines a surface in model parameter space, which is shown as a contour plot in Fig. 5. A wide range of "optimal" x_{Li} values are identified. With regard to real materials, the question is then, which regions of parameter space correspond to real materials, and to what degree the simple parameters considered here vary across possible chemistries of the garnet family. For example => discussion of effect of cation size / polarizabilities on conductivity trends? Larger cations: larger lattice parameter → decreased nearest-neighbour repulsion? Possibly modify balance of $\Delta E_{\mathrm{sites}}$? High polarisability? → increased screening? and reduced E_{nn}? Poses an interesting challenge: to what degree can effective parameters describing a simplified Hamiltonian (such as those employed here) be extracted from e.g. electronic structure calculations on real garnet materials?

IV. DISCUSSION

Summary. What was the motivation (A→B). What have we done to explore / solve this problem? What are notable results?

Summary → How well does this meet the goals laid out in the introduction?

=> To add above: nearest-neighbour interactions and relative site energies are possibly manipulated through the choice of lattice cations, because this determines lattice-site separations, and also the dielectric screening between adjacent Li ions.

Discuss the benefits / problems with this kind of model Hamiltonian analysis (speed / sampling of parameter space / direct interpretation of simple conceptual interactions) Shortcomings: barrierless kMC (all barriers could be quantified, but is there a straightforward way to map across interactions away from "known" materials? => cite relevant VdV / Ceder papers discussing e.g. variation in barriers with composition)

Other issues: assumption of a perfect lattice? (cf. Kozinsky / t-LLZO) Only single particle jumps (again t-LLZO shown to have many-particle jumps[43] also Sci. Rep. paper if published?)

Additional comment (re: Lucy) can invert this question: experimental data on maximum σ can be used to (qualitatively) estimate relative interaction energies by identifying model parameters that "best fit" experimen-

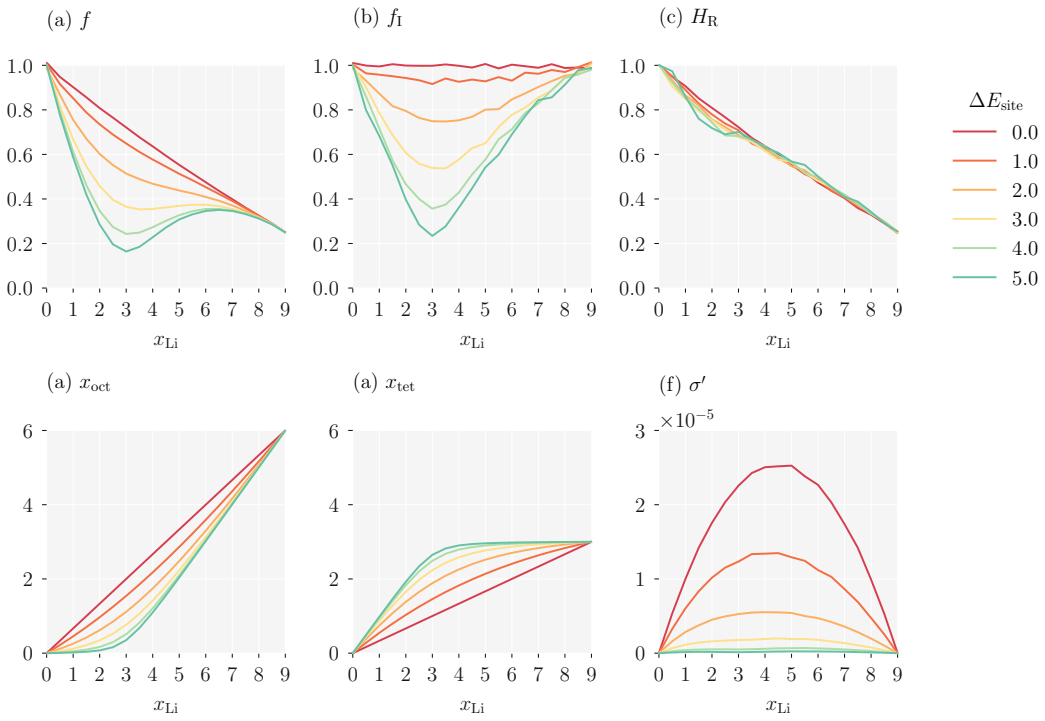

FIG. 4. The effect of unequal site occupation energies for mobile particles on a garnet lattice: (a) single-particle correlation factor, f; (b) collective correlation factor, f_{I}; (c) Haven ratio, H_{R}; (d) average octahedra occupation, x_{oct}; (e) average tetrahedra occupation, x_{tet}; (f) effective ionic conductivity, σ'. ΔE_{site} is in multiples of kT.

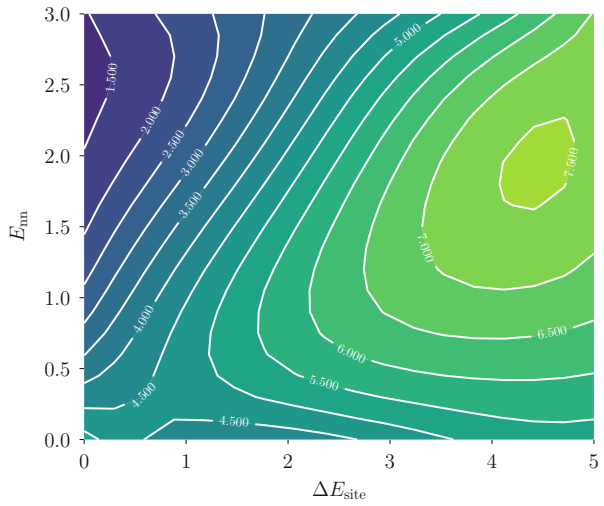

FIG. 5. CAPTION

tal data for specific materials. This fits with e.g. estimating model parameters from identifying those that reproduce known / predicted site occupations.

=> Discuss: Kozinsky *et al.* have also proposed a fully ordered phase at $x_{\mathrm{Li}} = 6$, from a combined first-principles calculations and group theory analysis[63], with mixed octahedral and tetrahedral occupation.

V. SUPPLEMENTARY MATERIAL

Supplementary material for this study is available as a GitHub repository[64]. This repository contains (1) the complete data set used to support the findings of this study, (2) example scripts for running `lattice_mc` simulations on a garnet lattice, and (3) a Jupyter notebook containing the code used to generate Figs. 2–9. The `lattice_mc` code is available under the MIT license[58].

VI. ACKNOWLEDGEMENTS

B. J. M. acknowledges support from the Royal Society (UF130329). B. J. M. would also like to thank M. Burbano and M. Salanne for stimulating discussions.

=> Check (and simplify) and document example simulation script in SI

VII. APPENDIX

Note that Murch describes physical correlation effects as "a manifestation of order. For example, an ion on a "right" position in an ordered structure which migrates to a "wrong" position will tend to reverse that jump".[10]

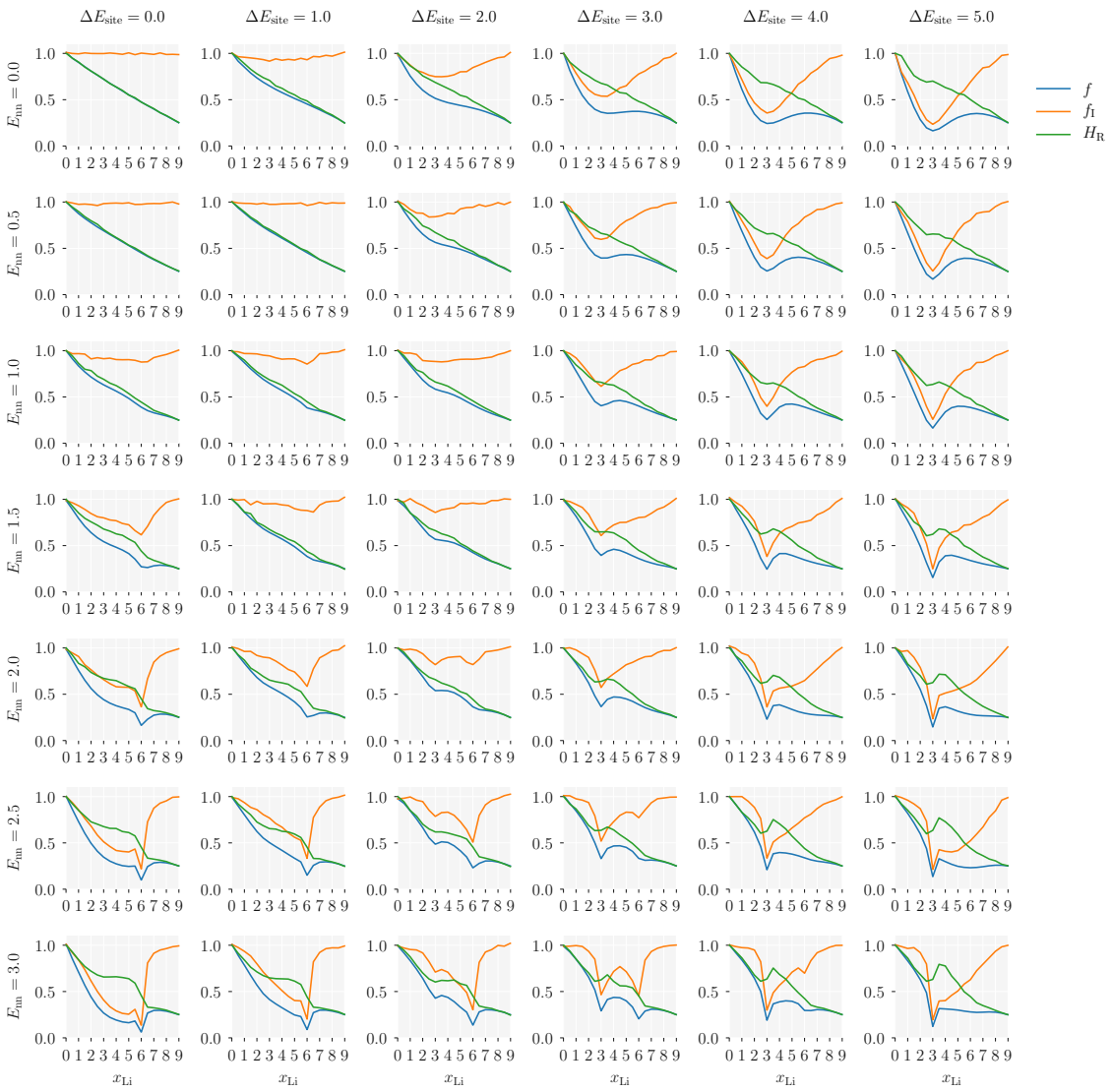

FIG. 6. CAPTION

[1] J. C. Bachman, S. Muy, A. Grimaud, H.-H. Chang, N. Pour, S. F. Lux, O. Paschos, F. Maglia, S. Lupart, P. Lamp, L. Giordano, and Y. Shao-Horn, Chem. Rev. **116**, 140 (2016).

[2] A. Manthiram, X. Yu, and S. Wang, Nat. Rev. Mater. **2**, 16103 (2017).

[3] J. B. Goodenough and P. Singh, J. Electrochem Soc. **162**, A2387 (2015).

[4] L. Malavasi, C. A. J. Fisher, and M. S. Islam, Chem. Soc. Rev. **39**, 4370 (2010).

[5] A. Van der Ven, J. Bhattacharya, and A. A. Belak, Acc. Chem. Res. **46**, 1216 (2013).

[6] Describing ionic transport as sequences of discrete hops breaks down for "super-ionic" solid electrolytes, with extremely mobile ions. The set of criteria for considering ionic transport to operate in a particle hopping regime are discussed by Catlow in C. R. A. Catlow, Sol. Stat. Ionics **8**, 89 (1983).

[7] The average hop rate per atom is the inverse of the mean residence time, $\widetilde{\nu} = 1/\widetilde{\tau}$. The contribution from each atom is a sum over individual hop rates, Γ_i, and is therefore related to the "total rate" of the kMC method via $\widetilde{\nu} = \langle Q \rangle / N$.[14].

[8] R. E. Howard and A. B. Lidiard, Rep Prog Phys. **27**, 161 (1964).

[9] A. M. Stoneham, ed., *Ionic Solids at High Temperatures* (World Scientific, 1989).

[10] G. E. Murch, Sol. Stat. Ionics **7**, 177 (1982).

[11] J. Bardeen and C. Herring, *Imperfections in Nearly Perfect Crystals* (John Wiley & Sons, Inc., 1952).

[12] K. Compaan and Y. Haven, Trans. Faraday Soc. **54**, 1498 (1958).

[13] A. R. Allnatt and A. B. Lidiard, *Atomic Transport in Solids* (Cambridge University Press, 2008).

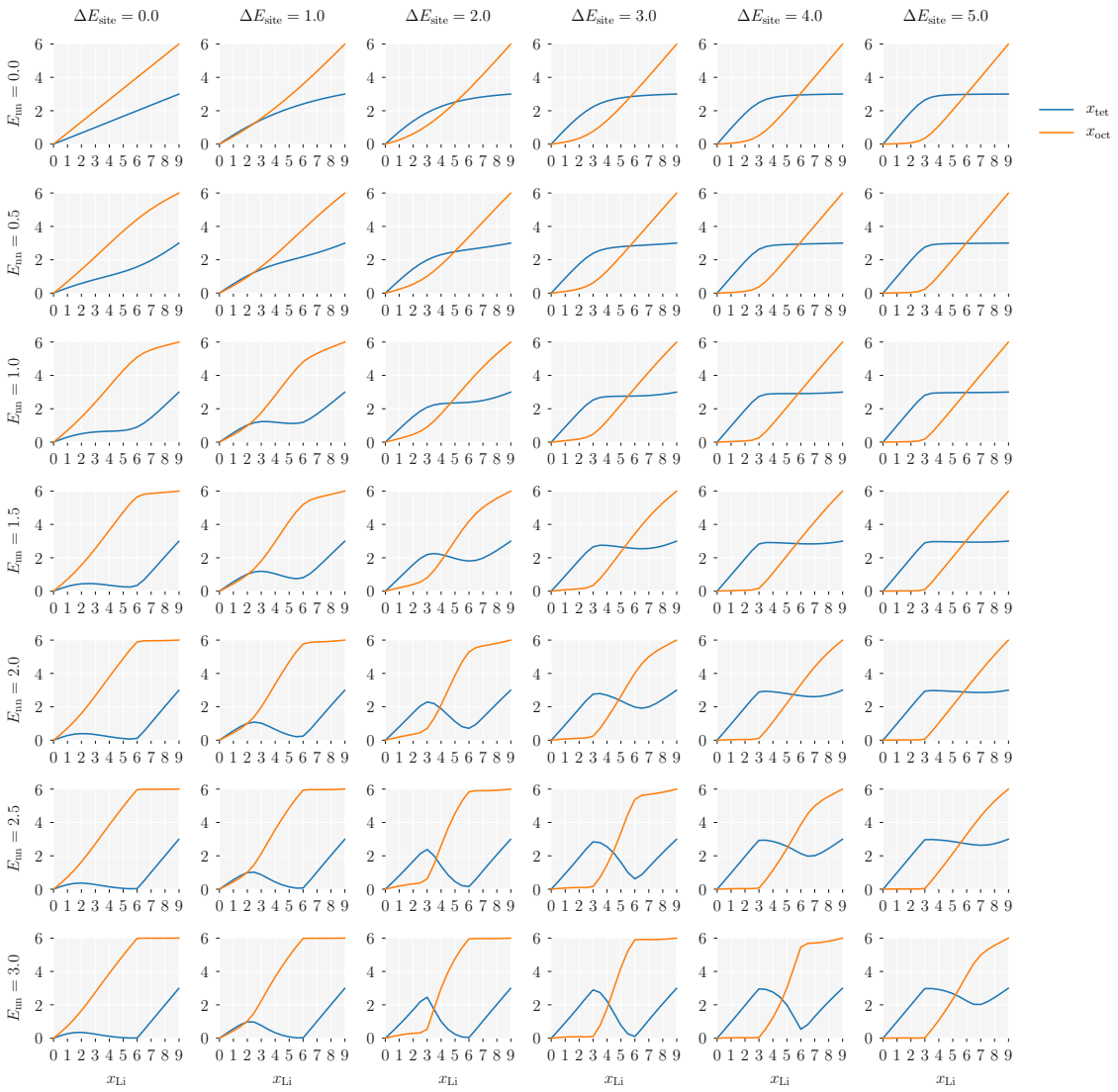

FIG. 7. CAPTION

[14] H. Mehrer (Springer, 2007).
[15] H. Sato and R. Kikuchi, J. Chem. Phys. **55**, 677 (1971).
[16] S. A. Akbar, J. Appl. Phys. **75**, 2851 (1994).
[17] M. Wilkening, W. Küchler, and P. Heitjans, Phys. Rev. Lett. **97**, 065901 (2006).
[18] B. Ruprecht, M. Wilkening, R. Uecker, and P. Heitjans, Phys. Chem. Chem. Phys. **14**, 11974 (2012).
[19] L. Enciso-Maldonado, M. S. Dyer, M. D. Jones, M. Li, J. L. Payne, M. J. Pitcher, M. K. Omir, J. B. Claridge, F. Blanc, and M. J. Rosseinsky, Chem. Mater. **27**, 2074 (2015).
[20] A. B. Santibáñez-Mendieta, C. Didier, K. K. Inglis, A. J. Corkett, M. J. Pitcher, M. Zanella, J. F. Shin, L. M. Daniels, A. Rakhmatullin, M. Li, M. S. Dyer, J. B. Claridge, F. Blanc, and M. J. Rosseinsky, Chem. Mater. **28**, 7833 (2016).
[21] H. Nozaki, M. Harada, S. Ohta, I. Watanabe, Y. Miyake, Y. Ikedo, N. H. Jalarvo, E. Mamontov, and J. Sugiyama, Sol. Stat. Ionics **262**, 585 (2014).
[22] M. Amores, T. E. Ashton, P. J. Baker, E. J. Cussen, and S. A. Corr, J. Mater. Chem. A **4**, 1729 (2016).
[23] R. D. Bayliss, S. N. Cook, S. Kotsantonis, R. J. Chater, and J. A. Kilner, Adv. Energy Mater. **4**, 1 (2014).
[24] W. G. Zeier, S. Zhou, B. Lopez-Bermudez, K. Page, and B. C. Melot, ACS Appl. Mater. Int. **6**, 10900 (2014).
[25] B. Lopez-Bermudez, W. G. Zeier, S. Zhou, A. J. Lehner, J. Hu, D. O. Scanlon, B. J. Morgan, and B. C. Melot, J. Mater. Chem. A **4**, 6972 (2016).
[26] A. Van der Ven, G. Ceder, M. Asta, and P. Tepesch, Phys. Rev. Lett. **64**, 184307 (2001).
[27] M. Mantina, Y. Wang, R. Arroyave, L. Q. Chen, Z. K. Liu, and C. Wolverton, Phys. Rev. Lett. **100**, 215901 (2008).
[28] B. J. Morgan and P. A. Madden, J. Phys-Condens. Matter **24**, 275303 (2012).
[29] R. J. Friauf, J. Appl Phys. **33**, 494 (1962).
[30] V. Thangadurai, H. Kaack, and W. Weppner, J. Am. Ceram. Soc. **86**, 437 (2003).
[31] V. Thangadurai, D. Pinzaru, S. Narayanan, and A. K. Baral, J. Phys. Chem. Lett. **6**, 292 (2015).

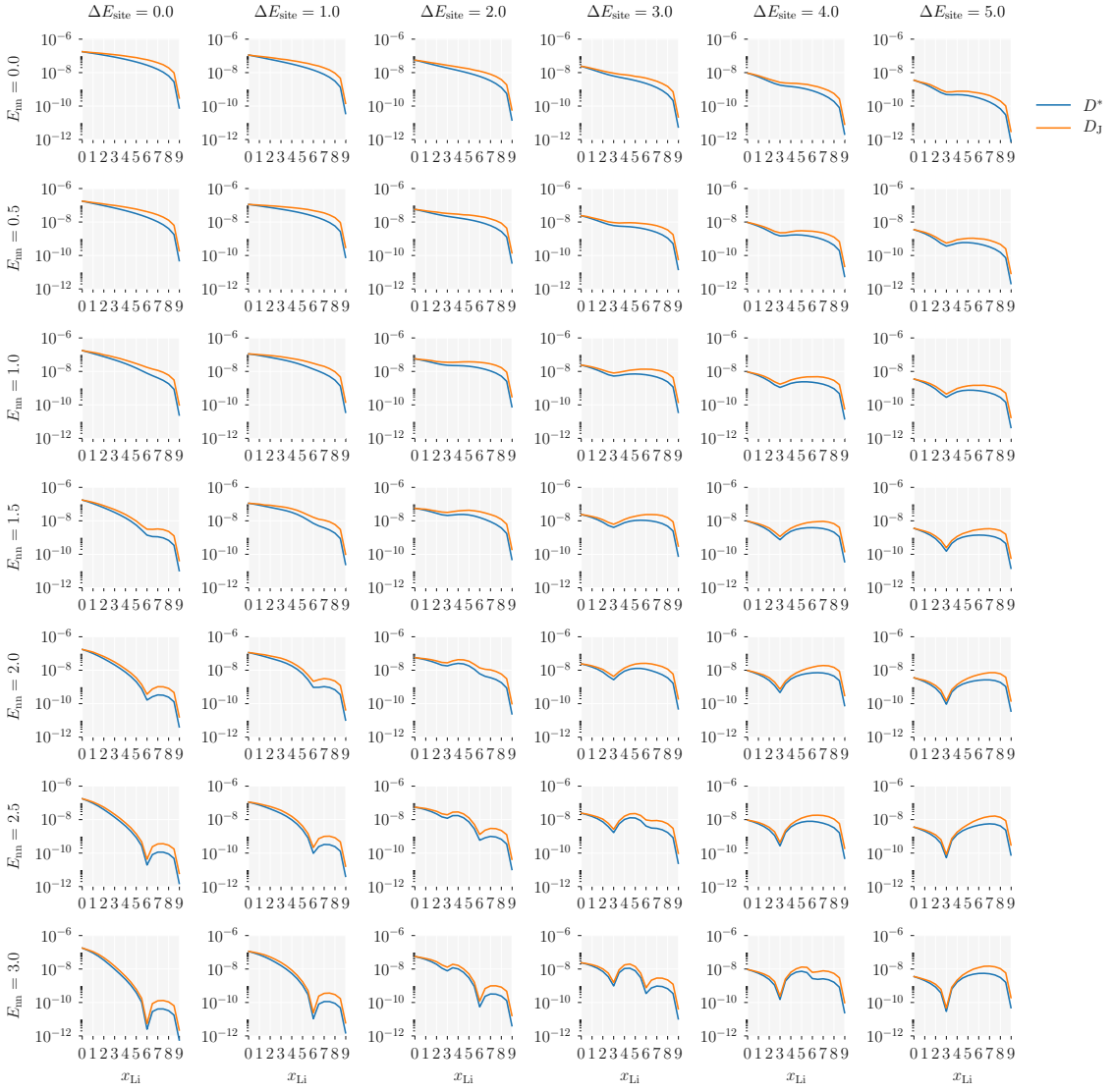

FIG. 8. CAPTION

[32] R. Inada, S. Yasuda, M. Tojo, K. Tsuritani, T. Tojo, and Y. Sakurai, Front. Energy Res. **4**, 336 (2016).
[33] J. Awaka, A. Takashima, K. Kataoka, N. Kijima, Y. Idemoto, and J. Akimoto, Chem. Lett. **40**, 60 (2011).
[34] M. P. O'Callaghan and E. J. Cussen, Chem. Comm. , 2048 (2007).
[35] M. P. O'Callaghan and E. J. Cussen, Sol. Stat. Sci **10**, 390 (2008).
[36] E. J. Cussen, J. Mater. Chem. **20**, 5167 (2010).
[37] Y. Wang, A. Huq, and W. Lai, Sol. Stat. Ionics **255**, 39 (2014).
[38] M. P. O'Callaghan, D. R. Lynham, E. J. Cussen, and G. Z. Chen, Chem. Mater. **18**, 4681 (2006).
[39] T. Thompson, A. Sharafi, and M. D. Johannes, Adv. Energy Mater. (2015).
[40] R. Jalem, Y. Yamamoto, H. Shiiba, M. Nakayama, H. Munakata, T. Kasuga, and K. Kanamura, Chem. Mater. **25**, 425 (2013).
[41] K. Meier, T. Laino, and A. Curioni, J. Phys. Chem. C (2014).
[42] M. Klenk and W. Lai, Phys. Chem. Chem. Phys. , 8758 (2015).
[43] M. Burbano, D. Carlier, F. Boucher, B. J. Morgan, and M. Salanne, Phys. Rev. Lett. **116**, 135901 (2016).
[44] M. J. Klenk and W. Lai, Sol. Stat. Ionics **289**, 143 (2016).
[45] M. Burbano, B. J. Morgan, and M. Salanne, "Li garnet md paper," In Preparation.
[46] A. Kuhn, S. Narayanan, L. Spencer, G. Goward, V. Thangadurai, and M. Wilkening, Phys. Rev. B **83**, 094302 (2011).
[47] A. Kuhn, V. Epp, G. Schmidt, S. Narayanan, V. Thangadurai, and M. Wilkening, J. Phys-Condens. Mat **24**, 035901 (2011).
[48] L. J. Miara, S. P. Ong, Y. Mo, W. D. Richards, Y. Park, J. M. Lee, H.-S. Lee, and G. Ceder, Chem. Mater. **25**, 3048 (2013).
[49] J. R. Rustad, arXiv (2016), related:H1H1zFMCzesJ.
[50] W. Gu, M. Ezbiri, R. P. Rao, M. Avdeev, and S. Adams, Sol. Stat. Ionics **274**, 100 (2015).
[51] S. Adams and P. P. Rao, J. Mater. Chem. **22**, 1426 (2012).

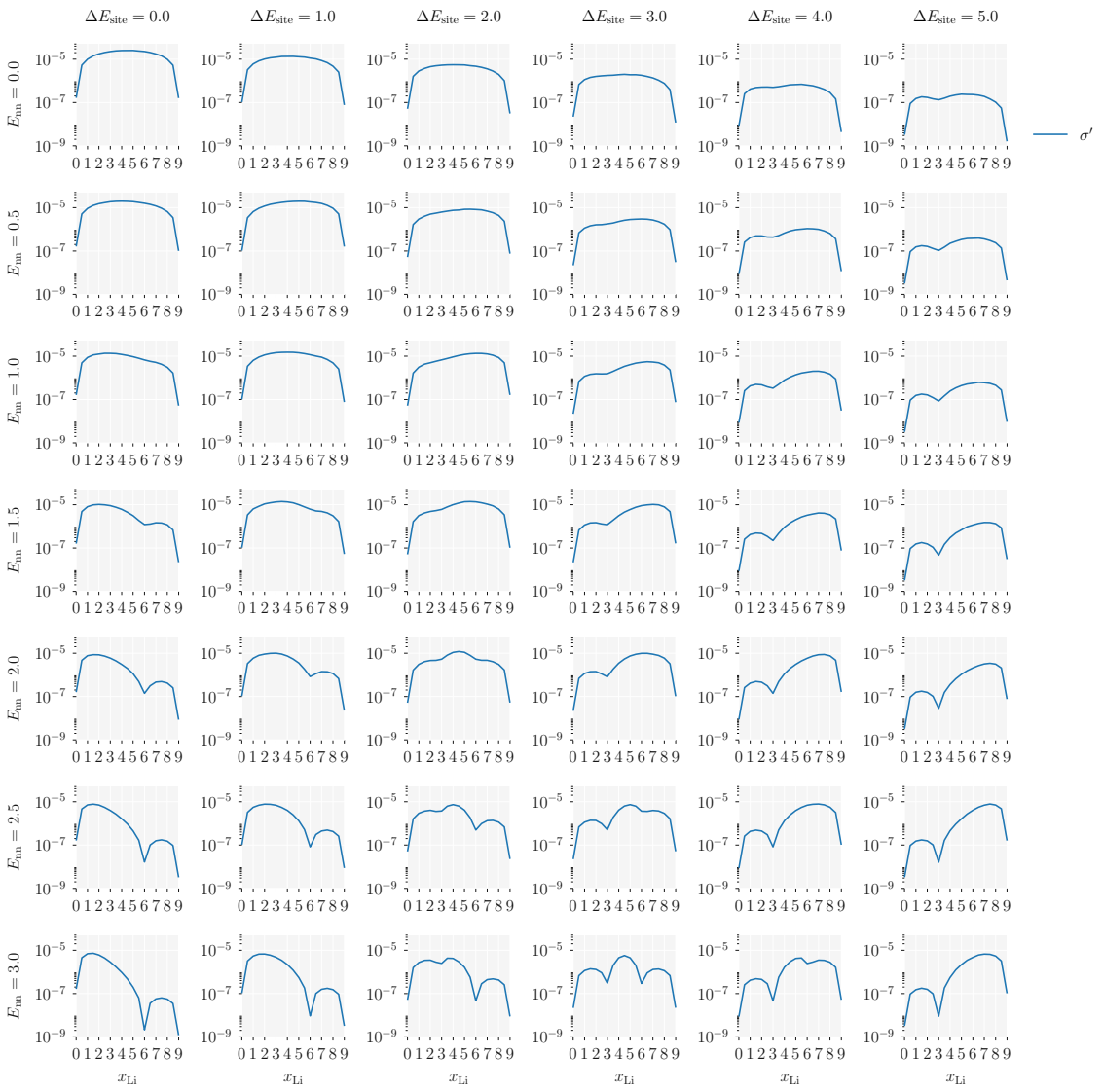

FIG. 9. CAPTION

[52] A. Düvel, A. Kuhn, L. Robben, M. Wilkening, and P. Heitjans, J. Phys. Chem. C **116**, 15192 (2012).

[53] S. Narayanan, V. Epp, M. Wilkening, and V. Thangadurai, RSC Adv. **2**, 2553 (2012).

[54] A. Ramzy and V. Thangadurai, ACS Appl. Mater. Int. **2**, 385 (2010).

[55] Here we follow the convention where "non-interacting" does not preclude volume-exclusion, where two mobile particles are forbidden from simultaneously occupying a single lattice site.[56] This definition is equivalent to all allowed configurations of particles having equal energies.

[56] R. Kutner, Phys. Lett. **81A**, 239 (1981).

[57] A. F. Voter, "Introduction to the kinetic monte carlo method," in *Radiation Effects in Solids*, edited by K. E. Sickafus, E. A. Kotomin, and B. P. Uberuaga (Springer Netherlands, Dordrecht, 2007) pp. 1–23.

[58] B. J. Morgan, J. Open Source Soft. **2** (2017), 10.21105/joss.00247.

[59] A linear least-squares fit to these data gives $R^2 = 0.9974$.

[60] K. Compaan and Y. Haven, Trans. Faraday Soc. **52**, 786 (1956).

[61] => Note that $\widetilde{\nu}$ is *not* the hopping prefactor used in these equations (there is a vacancy–coordination-number scaling)Because the lattice-gas model used here considers hops as barrierless, where hopping probabilities only depend on energy differences between intial and final states, the effective transport coefficients calculated here cannot be directly compared to experimental values. Introducing fixed barrier heights for tet↔oct hops is equivalent to scaling the hopping prefactor $\widetilde{\nu}$, which preserves *relative* differences in the transport coefficients presented here. A more realistic model would need to account for the influence of local site occupations on individual hopping barriers, see e.g. Ref.[65], and would give quantitative deviations from the trends presented here.

[62] For a system with a single mobile species, the reduced conductivity is equal to the true ionic conductivity if $(VkT)/(q^2) = 1$.

[63] B. Kozinsky, S. A. Akhade, P. Hirel, A. Hashibon, C. Elsässer, P. Mehta, A. Logéat, and U. Eisele, Phys. Rev. Lett. **116**, 055901 (2016).

[64] B. J. Morgan, "Lithium-garnet lattice-gas monte carlo dataset," `https://github.com/bjmorgan/garnet-lgmc-data` (2017).

[65] A. Van Der Ven and G. Ceder, in *Handbook of Materials Modelling* (2010) pp. 1–28.